

# Magnetic behavior of a new series of ternary compounds of the type, $R_2PtSi_3$ ( $R = La, Ce, Pr, Nd, Gd$ and $Y$ )

Subham Majumdar<sup>a</sup>, E.V. Sampathkumaran<sup>a,\*</sup>, M. Brando<sup>b</sup>,  
J. Hemberger<sup>b</sup>, A. Loidl<sup>b</sup>

<sup>a</sup>*Tata Institute of Fundamental Research, Homi Bhabha Road, Colaba, Mumbai 400005, India*

<sup>b</sup>*Experimentalphysik V, Elektronische Korrelationen und Magnetismus, Institut für Physik, Universität Augsburg, D-86135 Augsburg, Germany*

## 1. Introduction

In the recent past there has been considerable interest [1–11] in exploring the formation of new

ternary intermetallic compounds of the type  $R_2TX_3$  ( $R$  = rare earth,  $T$  = transition metal and  $X = Si, Ge$ ) and in studying their magnetic characteristics. As a continuation of our efforts in this direction [1–11], we report here the results of such a study on Pt-based compounds  $R_2PtSi_3$  ( $R = La, Ce, Pr, Nd, Gd$  and  $Y$ ). The main observations are: (i) while these compounds form in a

\*Corresponding author.

*E-mail address:* sampath@tifr.res.in  
(E.V. Sampathkumaran).

$\text{AlB}_2$ -derived hexagonal structure, there is a doubling of  $c$ -parameter for Gd and Y, but not for other members; (ii) the magnetic ordering of the moment-containing rare-earth ions (other than Pr, but including Ce) can be classified as a ferromagnetic-type; Pr compound exhibits complex magnetic properties; (iii) there is a breakdown of de Gennes scaling of magnetic ordering temperatures, not only for Ce, but also for Nd in this series and (iv) the Gd compound exhibits Kondo-lattice-like behavior in the electrical resistance data, presumably with a modulated magnetic structure at low temperatures.

## 2. Experimental details

The samples were prepared by arc melting stoichiometric amounts of constituent elements in an inert argon gas atmosphere. The ingots were then homogenized in an evacuated quartz tube at  $750^\circ\text{C}$  for two weeks. The X-ray diffraction patterns ( $\text{Cu K}\alpha$ ) confirm that all the samples form in an hexagonal  $\text{AlB}_2$  structure [8]. The heat-capacity ( $C$ ) measurements on these samples were performed in the temperature range 2–50 K using a semi-adiabatic heat pulse method. Magnetic susceptibility ( $\chi$ ) and isothermal magnetization ( $M$ ) measurements were measured using a commercial Vibrating Sample Magnetometer (Oxford Instruments) or a Superconducting Quantum Interference Device (Quantum Design). In addition, the AC  $\chi$  measurements for the Pr sample alone (2–25 K) with four different frequencies (1, 10, 100 and 1000 Hz) were also measured. The electrical resistivity ( $\rho$ ) measurements (2–300 K) were performed by a conventional four-probe technique with conducting silver paint for making electrical contacts.

## 3. Results and discussion

We first remark on a crystallographic feature on the basis of the present X-ray diffraction patterns (Fig. 1). The point of note is that additional weak lines are observed for the Gd alloy when compared with other members of this series, which are

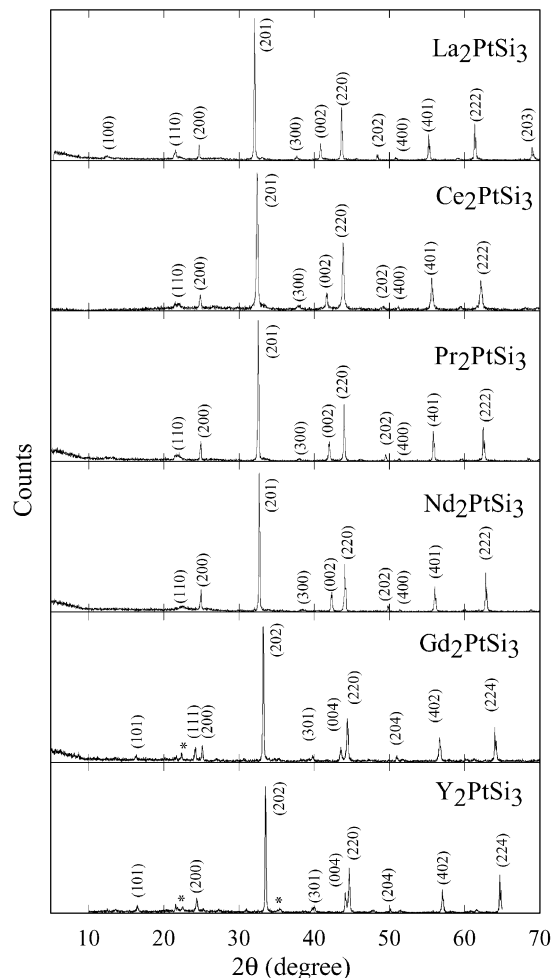


Fig. 1. X-ray diffraction patterns ( $\text{Cu K}\alpha$ ) for the compounds  $\text{R}_2\text{PtSi}_3$  ( $\text{R} = \text{La}, \text{Ce}, \text{Pr}, \text{Nd}, \text{Gd}$  and  $\text{Y}$ ) in the range  $2\theta = 5\text{--}70^\circ$ . The unindexable lines in  $\text{Gd}_2\text{PtSi}_3$  and  $\text{Y}_2\text{PtSi}_3$  are marked by an asterisk.

indexable if one assumes that there is a doubling of the unit-cell parameter  $c$  only for Gd; the diffraction patterns also suggest that  $a$  is found to be doubled for all the members from the observation of corresponding superstructure lines. We have also synthesised analogous Y sample, the X-ray diffraction pattern of which suggests doubling of  $c$ -axis. Thus, it appears that the size of the R ion plays a crucial role on the doubling of  $c$ -axis. The lattice constants were determined from the X-ray powder diffraction patterns (in the range of  $2\theta = 40\text{--}70^\circ$ ), which are shown in Table 1. While the

Table 1

The lattice parameters ( $a$ ,  $c$ ), unit-cell volume ( $V$ ), effective magnetic moment ( $\mu_{\text{eff}}$ ), paramagnetic Curie temperature ( $\Theta_p$ ) above 100 K (denoted by HT) and in the low-temperature range (LT, say in the range 20–30 K) just above magnetic ordering, and Curie temperature ( $T_C$ ) for the ternary compounds,  $R_2\text{PtSi}_3$

$R$	$a$ (Å)	$c$ (Å)	$V$ (Å <sup>3</sup> )	$\mu_{\text{eff}}$ ( $\mu_B$ )	HT $\Theta_p$ (K)	LT $\Theta_p$ (K)	$T_C$ (K)
La	8.290	4.417	262.87	—	—	—	—
Ce	8.250	4.332	255.40	2.57	−12	2	5
Pr	8.230	4.300	252.23	3.7	−5.4	−5.6	?
Nd	8.217	4.282	250.39	3.7	4.8	14	18
Gd	8.139	8.303	476.25	8.2	37	25	24
Y	8.099	8.194	465.42	—	—	—	—

doubling of ‘ $a$ ’ arises from crystallographic ordering of Pt and Si ions, the one of ‘ $c$ ’ could be from a slight distortion of the R-plane as seen for  $\text{Er}_2\text{RhSi}_3$  [9].

For  $\text{La}_2\text{PtSi}_3$ , while the value of  $\chi$  is very small ( $5 \times 10^{-3}$  emu/mol at 300 K), we observe a Curie–Weiss behavior as a function of temperature, which may be attributed to some paramagnetic impurities, e.g., estimated Ce impurity of about 0.1%. The  $C$  data are shown in Fig. 2 along with the data for Ce compound. The results basically establish that  $\text{La}_2\text{PtSi}_3$  is not superconducting down to 2 K and that Pt does not carry any magnetic moment.

The  $\rho$ ,  $\chi$ ,  $M$  and  $C$  data for the compound  $\text{Ce}_2\text{PtSi}_3$  are shown in Figs. 2 and 3. In the plot of  $C$  vs.  $T$  data, we see a  $\lambda$ -type of anomaly at low temperatures with a sharp upturn below 5 K establishing the existence of a long-range magnetic ordering at this temperature. In support of this conclusion, in the plot of  $\rho$  vs.  $T$  data, we observe a drop in  $\rho$  around this temperature due to the loss of spin-disorder contribution (Fig. 2). It is important to note that there is no prominent minimum in the plot of  $\rho$  vs.  $T$ , particularly at low temperatures before the onset of long-range magnetic order, which appears to suggest that the Kondo effect is weak at such temperatures in this compound. The plot of inverse  $\chi$  vs.  $T$  measured in a field of 5 kOe shows a distinct change in the slope around 5 K (see Fig. 2) due to magnetic order; also, the zero-field-cooled (ZFC)  $\chi$  measured in a low field of 50 Oe exhibits a distinct deviation from field-cooled (FC)  $\chi$  data around 5 K, which is attributable to anisotropy and grain-boundary

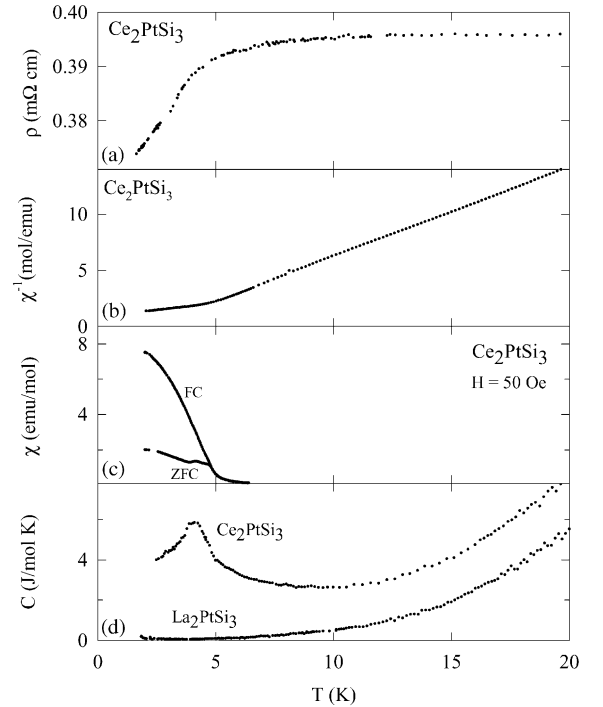


Fig. 2. (a) The electrical resistivity ( $\rho$ ), (b) inverse susceptibility ( $\chi$ ) ( $H = 5$  kOe), (c)  $\chi$  taken at 50 Oe for the zero-field-cooled (ZFC) and field-cooled (FC) state of the specimen and (d) heat capacity ( $C$ ) as a function of temperature below 20 K for  $\text{Ce}_2\text{PtSi}_3$ . The  $C$  data for the La compound is also included in the figure.

effects, often seen in ferromagnets as well. The isothermal  $M$  measured at 2 K tends to saturate at high fields (Fig. 3, inset) and the value of the saturation moment is about  $1 \mu_B/\text{Ce}$ , similar to that expected for the doublet ground state of Ce;

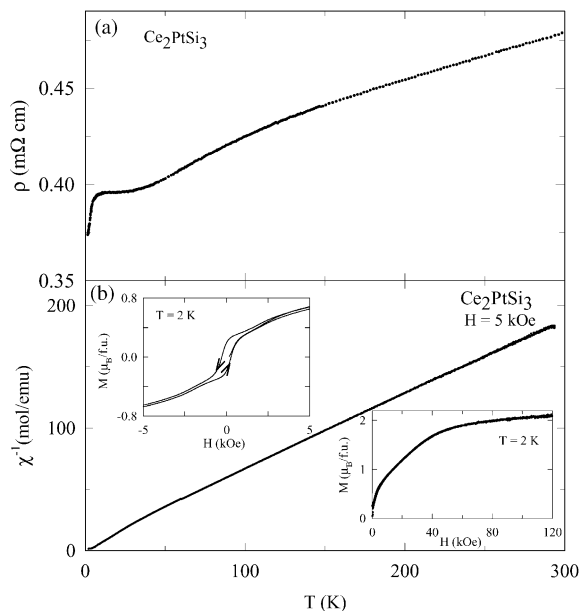


Fig. 3. (a) The electrical resistivity ( $\rho$ ) and (b) inverse susceptibility ( $\chi$ ) (taken in a field of 5 kOe) vs. temperature for  $\text{Ce}_2\text{PtSi}_3$  in the temperature range 2–300 K. Isothermal magnetization up to 120 kOe and the hysteresis loop (+5 to  $-5$  Oe) are also shown as insets in (b).

in addition, the variation of  $M$  with  $H$  shows hysteresis (see inset of Fig. 3). These findings suggest that this Ce compound can be classified as a ferromagnet. A careful look at the low-field side of the hysteresis plot, however, suggests that there may be a weak metamagnetic transition around 500 Oe, thereby indicating the presence of an antiferromagnetic component or a canting of magnetic moments in zero magnetic field. The plot of inverse  $\chi$  vs.  $T$  is found to be linear above 50 K and the value of the effective magnetic moment ( $\mu_{\text{eff}} = 2.57 \mu_{\text{B}}$ ) is typical of trivalent Ce ions; the value of the Curie–Weiss temperature ( $\Theta_{\text{p}}$ ) from this linear region is found to be  $-12$  K; the negative sign with a magnitude much larger than the magnetic transition temperature indicates the existence of the Kondo correlations at high temperatures (that is, when all the crystal-field levels are occupied), which apparently vanishes at low temperatures following the occupation of low-lying crystal-field levels as also indicated by positive  $\Theta_{\text{p}}$  ( $+2$  K) below 15 K (see Fig. 2). With the magnetic ordering dominating over the Kondo

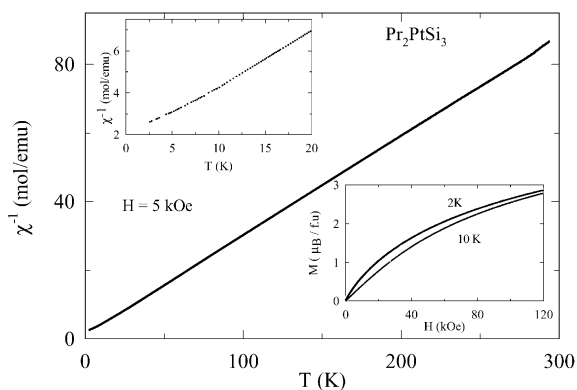


Fig. 4. Inverse magnetic susceptibility ( $\chi$ ) ( $H = 5$  Oe) as a function of temperature in the range 2–300 K for  $\text{Pr}_2\text{PtSi}_3$ . The low-temperature data in an expanded form and isothermal magnetization ( $M$ ) at 2 and 10 K are shown as insets.

effect, we infer that this compound is placed below or at the peak of the well-known Doniach’s magnetic phase diagram. It is of interest to perform high-pressure studies to verify this proposal.

In Fig. 4, we depict  $\chi$  ( $H = 5$  kOe) and  $M$  data for the compound  $\text{Pr}_2\text{PtSi}_3$ . The plot of inverse  $\chi$  vs.  $T$  plot is linear down to about 15 K; the value of  $\mu_{\text{eff}}$  is found to be  $3.7 \mu_{\text{B}}$ , which is close to that expected for trivalent Pr ions and the value of  $\Theta_{\text{p}}$  is found to be  $-5.4$  K. There is a change in slope (Fig. 4, inset) around 15 K as the  $T$  is lowered below 20 K. In order to understand this aspect further, we have measured low field ( $H = 50$  Oe)  $\chi$  behavior (Fig. 5) and we note that there is a distinct anomaly near 15 K with ZFC–FC  $\chi$  deviation indicating the possibility of an onset of magnetic order; in addition,  $\chi$  exhibits an upturn below about 7 K indicating the possibility of another magnetic transition. However, other experimental results do not favor the presence of long-range magnetic ordering in this system. For instance, in the raw  $C$  data (Fig. 5), we observe a broad shoulder around 10 K, however without any evidence for a prominent  $\lambda$ -type of anomaly. There is also a continuous change in slope around 15 K, without a well-defined drop, in  $\rho$  data. While these findings appear to favor a proposal in terms of spin-glass-freezing (arising due to crystallographic disorder between Pt and Si sites), the AC  $\chi$  data do

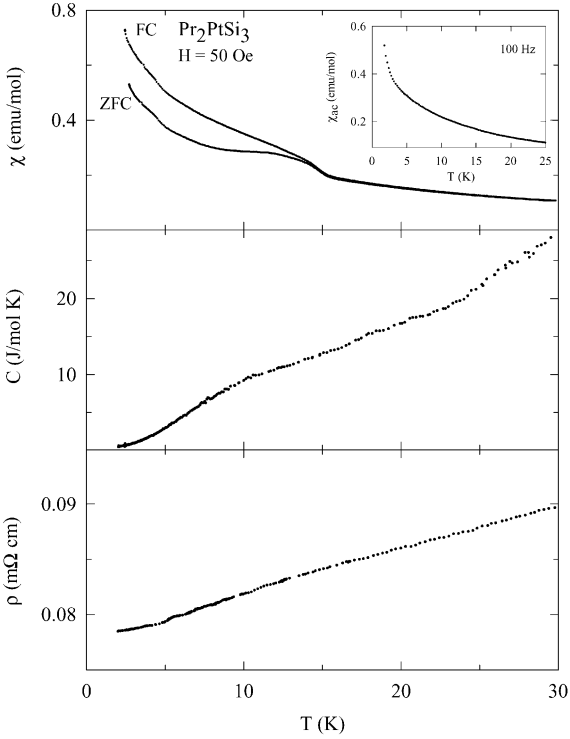


Fig. 5. Low-field ( $H = 50$  Oe) magnetic susceptibility ( $\chi$ ), heat capacity ( $C$ ) and electrical resistivity ( $\rho$ ) below 30 K for  $\text{Pr}_2\text{PtSi}_3$ . Typical low-temperature AC  $\chi$  behavior is shown in the inset.

not favor the existence of any type of magnetic ordering; that is, AC  $\chi$  measured at different frequencies (see Fig. 5, inset) shows a continuous rise with decreasing temperature without any evidence of a cuspland without showing any frequency dependence. Thus, the observed properties of this compound are difficult to understand consistently. It is not clear at present whether small undetectable amount of magnetic impurities are responsible for the DC  $\chi$  anomalies around 15 K, while the broad feature in  $C$  around 10–15 K is due to Schottky anomalies; in other words, with this line of arguments, this compound could be intrinsically non-magnetic down to 2 K. Alternatively, the Pr ions at the minority site [4] may be ordering magnetically, while  $\chi$  of remaining non-magnetic Pr ions are so large that the features due to minority Pr ion magnetic ordering is missed in the AC  $\chi$  data. More measurements are required to clarify the magnetism of this compound. Finally,

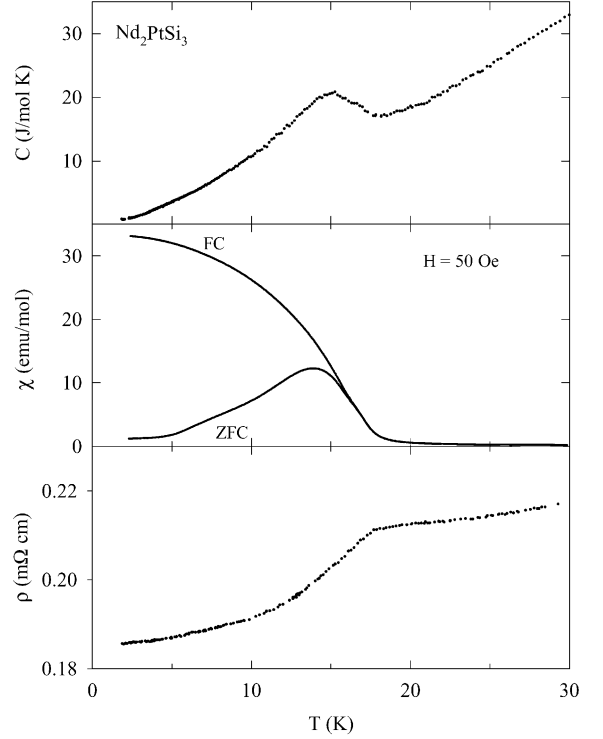


Fig. 6. Heat capacity ( $C$ ), magnetic susceptibility ( $\chi$ ) taken in a field of 50 Oe for the ZFC and FC conditions of the specimens, and electrical resistivity ( $\rho$ ) in the temperature range 2–30 K for  $\text{Nd}_2\text{PtSi}_3$ .

the plots of isothermal  $M$  at 2 and 10 K look similar with a sluggish tendency towards saturation at higher fields.

With respect to  $\text{Nd}_2\text{PtSi}_3$ , Figs. 6–8 bring out the temperature-dependent behavior of measured properties. The  $C$  data clearly show (Fig. 6) an upturn below 18 K with a well-defined peak at 15 K. The  $\chi$  data ( $H = 50$  Oe) also show a sharp rise below 18 K, with the FC and ZFC  $\chi$  measured in a field of 50 Oe deviating below 15 K. There is also a corresponding drop in the  $\rho$  vs.  $T$  plot at about 17.5 K as  $T$  is lowered. These results establish that long-range magnetic ordering sets in below 18 K in this compound. The plot of an isothermal magnetization at 2 K exhibits hysteretic behavior, which establishes that the magnetic ordering of Nd ions is of a ferromagnetic-type. From the Curie–Weiss region in the plot of inverse  $\chi$  vs.  $T$  above 50 K, we find that the sign of  $\Theta_p$  is positive (4.8 K),

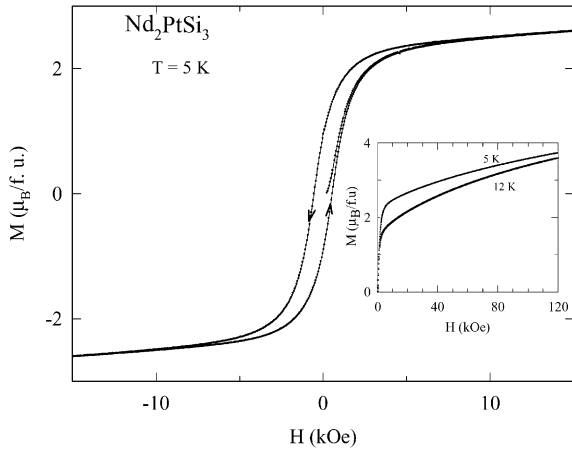


Fig. 7. Hysteresis loop at 5 K for  $\text{Nd}_2\text{PtSi}_3$ . The isothermal magnetization behavior at 5 and 12 K are shown in the inset.

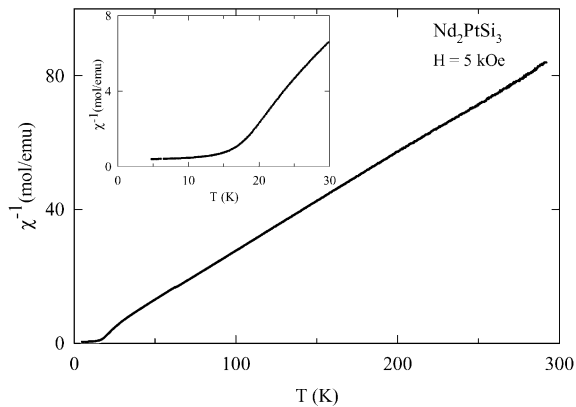


Fig. 8. Inverse magnetic susceptibility ( $\chi$ ) ( $H = 5$  Oe) as a function of temperature in the range 2–300 K for  $\text{Nd}_2\text{PtSi}_3$ . The low-temperature data in an expanded form is shown in the inset.

consistent with ferromagnetic ordering and the magnitude below 30 K becomes comparable to that of  $T_C$ ; (the value of the  $\mu_{\text{eff}}$  ( $3.70 \mu_B$ ) derived from the above linear region is consistent with trivalency of Nd ion). It may be remarked that isothermal  $M$  in Fig. 7 exhibits a sharp rise at low fields, but it does not show any tendency for saturation even at a field as high as 120 kOe. This clearly shows that this composition is also presumably characterized by a complex ferromagnetic structure or the Nd ions at one of the two sites [8] which remain paramagnetic down to 5 K.

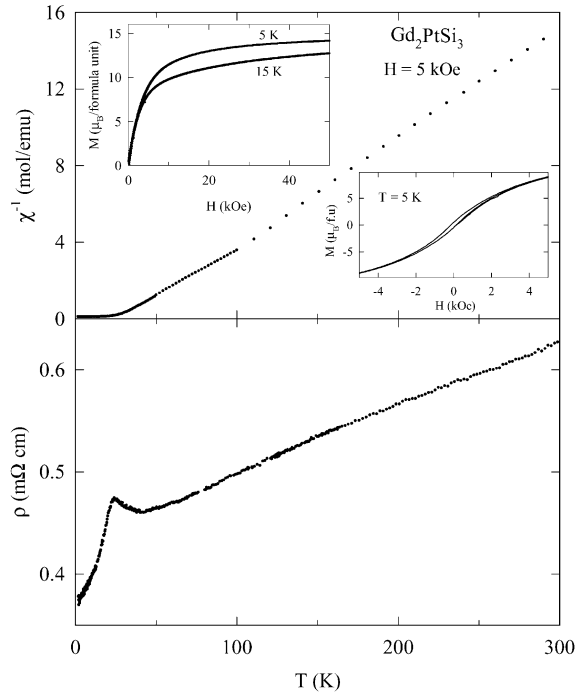


Fig. 9. Inverse susceptibility ( $\chi$ ) ( $H = 5$  Oe) and electrical resistivity ( $\rho$ ) in the temperature range 2–300 K for  $\text{Gd}_2\text{PtSi}_3$ . Isothermal magnetization ( $M$ ) behavior at 5 and 15 K upto 50 kOe and hysteresis loop at 5 K are shown as insets.

The Y compound is found to be neither superconducting nor magnetic in the  $T$  range of investigation. The results on the Gd alloy are shown in Figs. 9 and 10. While the compound is found to be paramagnetic above 24 K as suggested by the  $\chi$  data, there is a sharp upturn in  $\chi$  below 25 K in the data recorded in an applied magnetic field of 5 kOe, indicating the onset of ferromagnetic ordering near 24 K. The FC and ZFC  $\chi$  obtained at  $H = 50$  Oe exhibit a deviation below 24 K, consistent with the onset of magnetic ordering at this temperature. The ordering is of a ferromagnetic-type and the observations supporting this are that the sign of  $\Theta_p$  is found to be positive not only above 125 K but also at lower temperatures (37 and 25 K respectively); isothermal  $M$  almost exhibits saturation at higher fields both at 5 and 15 K, with the value of the saturation moment, say at 5 K, the same as that expected for Gd ion; the variation of  $M$  vs.  $H$  is hysteretic. The

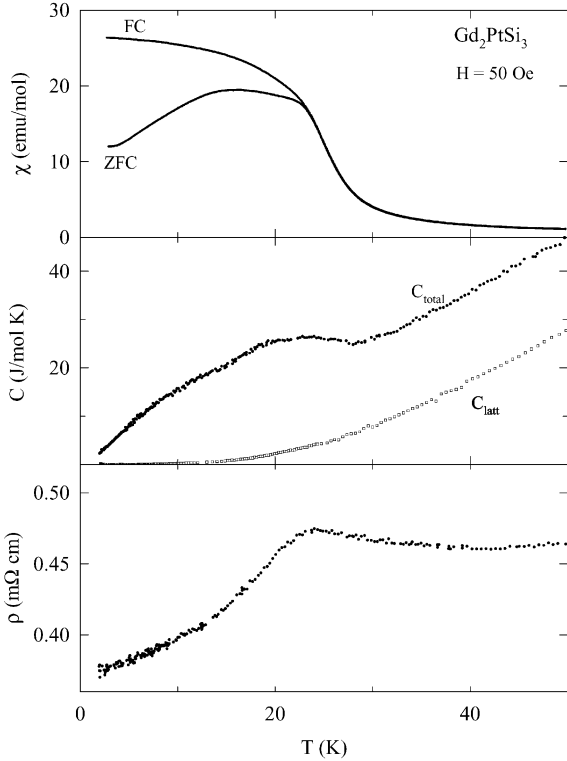


Fig. 10. Low-field (50 Oe) magnetic susceptibility ( $\chi$ ) for FC and ZFC state of the specimen, heat capacity ( $C$ ) and electrical resistivity ( $\rho$ ) behavior in the temperature range 2–50 K for  $\text{Gd}_2\text{PtSi}_3$ . The  $C$  data for  $\text{Y}_2\text{PtSi}_3$  after scaling for differences in Debye temperatures with the Gd compound as per the procedure given by Blanco et al. [12–14] are also shown as  $C_{\text{latt}}$ .

$C$  data also show an anomaly in the vicinity of  $T_C$ , however, the peak is broadened. A careful look at the peak value renders additional information on the nature of ferromagnetic ordering. It is a well-known fact [12–14] that, for the Gd alloys with equal magnetic structure, the peak value of the 4f-contribution to  $C$  should be  $20.15 \text{ J/Gd mol K}$  and any reduction from this value arises from the modulation of magnetic structure; in the present case, even without the subtraction of the lattice part, the peak value (per Gd) is much less (close to  $15 \text{ J/Gd mol K}$ ); this establishes that there must be some modulation of the ferromagnetic structure and it is of interest to carry out further studies to understand this aspect better. It may be stated that we attempted to derive the 4f contribution ( $C_{4f}$ ) to

$C$  employing the values of the Y compound as suggested by Blanco et al. [12–14] however, in this case, this method of deriving  $C_{4f}$  failed as the total magnetic entropy keeps increasing beyond theoretically expected value of  $R \ln 8 \text{ J/Gd mol K}$ ; this is also obvious from the fact that the curve  $C_{\text{latt}}$  in Fig. 10 runs parallel to the plot of  $C$  vs.  $T$  data of Gd compound. With respect to the magnetic behavior in the paramagnetic state it may be noted that the plot of inverse  $\chi$  vs.  $T$  exhibits Curie–Weiss behavior only down to about 125 K, below which there is a deviation from linearity; this deviation cannot be attributed to crystal-field effects, as Gd is an S-state ion and therefore we believe that the magnetic precursor effects [15] are operative over a wide temperature range above  $T_C$ . In support of this, the plot of  $\rho$  versus  $T$  exhibits a prominent minimum around 40 K (typical of that expected for Ce/U-based magnetically ordered Kondo lattices), similar to that noted for  $\text{Gd}_2\text{PdSi}_3$  (Ref. [1]) and  $\text{Gd}_2\text{CuGe}_3$  (Ref. [6]). This kind of transport behavior is unusual, as it is well-known that Gd ions do not exhibit the Kondo effect due to well-localized nature of the 4f orbital and the temperature derivative of  $\rho$  should be positive in the paramagnetic state for such metallic systems; further discussion in this regard can be found in Ref. [15]. Finally, the value of  $\mu_{\text{eff}}$  obtained from the high-temperature linear region is found to be  $8.2 \mu_B/\text{Gd}$ , which is marginally higher ( $0.2 \mu_B$ ) than the theoretically expected value presumably due to conduction electron polarization.

#### 4. Summary

We have synthesized new class of ternary rare-earth compounds of the type  $\text{R}_2\text{PtSi}_3$  for  $\text{R} = \text{La}, \text{Ce}, \text{Pr}, \text{Nd}, \text{Gd}$  and  $\text{Y}$ . We have not attempted to synthesize other members of this series. While, we found that these compounds form in an  $\text{AlB}_2$ -derived hexagonal structure, apparently there is a dependence of the superstructure formation (doubling of  $c$ -axis) on the size of R as indicated by X-ray diffraction, with La, Ce, Pr and Nd belonging to a structure without doubling of  $c$  and Gd and Y belonging to the other class. All the

magnetic-moment-containing R compounds at low temperatures behave like ferromagnets (except the Pr compound), with the magnetic transition temperatures Ce and Nd (5 and 18 K, respectively) much larger than that expected on the basis of de Gennes scaling. All the presently available data for the Pr compound is difficult to interpret consistently in terms of the existence of a magnetic ordering at low temperatures. We find distinct evidence from the  $C$  data for a modulation of magnetic structure for the Gd compound. Interestingly, the Gd compound is identified to be a Gd alloy (third among the ones) exhibiting resistivity minimum, in spite of the fact that, even in the case of the Ce compound, such a minimum is absent signalling the weakening of the Kondo effect at low temperatures. The Ce compound adds to a small list [16–18] of ferromagnetic Ce compounds with negligible effect of the Kondo effect in the magnetically ordered state and we hope this finding will be useful for systematic understanding of the competition phenomena (between magnetism and the Kondo effect). We call for detailed neutron diffraction studies on these interesting class of materials in order to understand the exact nature of magnetic structure.

## References

- [1] R. Mallik, E.V. Sampathkumaran, M. Strecker, G. Wortmann, *Europhys. Lett.* 41 (1998) 315.
- [2] R. Mallik, E.V. Sampathkumaran, P.L. Paulose, *Solid State Commun.* 106 (1998) 169.
- [3] A. Szytula, M. Hofmann, B. Penc, M. Slaski, S. Majumdar, E.V. Sampathkumaran, A. Zygmunt, *J. Magn. Magn. Mater.* 202 (1999) 365.
- [4] R. Mallik, E.V. Sampathkumaran, M. Strecker, G. Wortmann, P.L. Paulose, Y. Ueda, *J. Magn. Magn. Mater.* 185 (1998) L135.
- [5] S. Majumdar, R. Mallik, E.V. Sampathkumaran, P.L. Paulose, K.V. Gopalakrishnan, *Phys. Rev. B* 59 (1999) 4244.
- [6] S. Majumdar, E.V. Sampathkumaran, *Phys. Rev. B* 61 (2000) 43 and references therein.
- [7] E.V. Sampathkumaran, I. Das, R. Rawat, S. Majumdar, *Appl. Phys. Lett.* 77 (2000) 418.
- [8] R.A. Gordon, C.J. Waren, M.G. Alexander, F.J. DiSalvo, R. Pöttgen, *J. Alloys Compounds* 248 (1997) 24.
- [9] P.A. Kotsanidis, J.K. Yakinthos, E. Gamari-Seale, *J. Magn. Magn. Mater.* 87 (1990) 199.
- [10] B. Chevalier, et al., *Solid State Commun.* 49 (1984) 753.
- [11] S. Majumdar, E.V. Sampathkumaran, *Phys. Rev. B* 62 (2000) 8959.
- [12] J.A. Blanco, D. Gignoux, D. Schmitt, *Phys. Rev. B* 43 (1991) 13145.
- [13] J.A. Blanco, D. Gignoux, P. Morin, D. Schmitt, *Europhys. Lett.* 15 (1991) 671.
- [14] M. Bouvier, P. Lethuillier, D. Schmitt, *Phys. Rev. B* 43 (1991) 13137.
- [15] R. Mallik, E.V. Sampathkumaran, *Phys. Rev. B* 58 (1998) 9178 and references therein.
- [16] I. Das, E.V. Sampathkumaran, *Phys. Rev. B* 48 (1993) 16103.
- [17] I. Das, E.V. Sampathkumaran, *Physica B* 205 (1995) 259.
- [18] E.V. Sampathkumaran, I. Das, *J. Magn. Magn. Mater.* 147 (1995) L240.